REGULAR ARTICLE

An empirical, variational method of approach to unsymmetric valley-ridge inflection points

Wolfgang Quapp · Benjamin Schmidt

Abstract Valley-ridge inflection points (VRIs) emerge on a potential energy surface of a chemical reaction if the reaction pathway bifurcates. The valley of the reaction path branches into two valleys, and a ridge in between. It can happen in uphill or in downhill direction. Newton trajectories (NT) are curves for the description of the reaction path. They are curves where at every point the gradient of the potential energy surface points into the same direction. Singular Newton trajectories are a special case: they bifurcate at VRI points. To find a singular Newton trajectory is quasi equivalent with the determination of the corresponding VRI point where this NT bifurcates. Often the bifurcation of the reaction path is governed by a symmetry of the problem. Then the symmetry axis is usually the first branch of the singular NT, and so its determination is easy. In case of an unsymmetric branching, however, such a guiding line is missing. We name the place of such a bifurcation a skew VRI. We propose a variational calculation of the singular NT through the VRI of interest by an empirical, iterative method. Before, the variational theory of possible reaction pathways is developed and applied to the intrinsic reaction coordinate (IRC), as well as to NTs. We have to employ the theory of NTs with its many facets, we use especially the Branin equation. The developed method is applied to the calculation of VRI points on the potential energy surface of HCN and to a VRI point of alanine dipeptide being adjacent to the C5 minimum.

1 Introduction

The concept of the Newton trajectory (NT) builds a static model of a reaction path (RP) of an adiabatic potential energy surface (PES) [1, 2, 3, 4, 5, 6, 7]. It is a side approach to the theoretical kinetics of chemical systems [8]. An RP is roughly defined as a line in the coordinate space, which connects two minimizers by passing the saddle point (SP), the transition state (TS) structure or a "mountain pass" of an adiabatic PES following the valley [9]. The energy of the SP is assumed to be the highest value tracing along the RP. It is the minimal energy a reaction needs to take place. Reaction theories are based on the knowledge of the RP either implicitly (transition state theory [10, 11]) or explicitly (variational transition state theory [8, 12]). These theories only require local information about the PES along the RP. They circumvent the dimension problem: it is impossible to fully calculate the PES. Because this is the fundamental problem in handling an n-dimensional hypersurface, it is the large dimension. Molecules with more than $N = 4$ atoms would cause an overwhelming number of net points for the PES. The RP concept is a promising way out. It reduces the problem of finding an algorithm for one-dimensional curves—without any knowledge of the whole PES. A parameterization t of the RP $\mathbf{x}(t) = (x^1(t), \ldots, x^n(t))^T$ is called *reaction coordinate*.

The SP and the minimums form stationary points of the PES. Roughly speaking, it is only of secondary interest, how a reaction path ascends to the SP. This looseness

W. Quapp (✉) · B. Schmidt
Mathematical Institute, University of Leipzig,
Johannis-Gasse 26, PF 10 09 20, 04009 Leipzig, Germany
e-mail: quapp@uni-leipzig.de
URL: http://www.math.uni-leipzig.de/~quapp/

makes possible a variety of RP definitions, thus, instead of the usually used steepest descent for the minimum energy path (MEP), we may use an NT which has to monotonously connect a minimum and an SP to be an RP [13], thus we have to exclude NTs which have a turning point with an energy higher than the SP. An NT is a curve where a selected gradient direction equally comes out at every curve point. There are NTs, which in most cases pass all stationary points. Thus, NTs are an interesting procedure in order to determine all types of stationary points [1] by way of trial. Besides the RP-property, NTs can be used to define and find some kinds of valley-ridge inflection (VRI) points [2, 6], because they bifurcate there. The interest in skew VRI points has increased in the last time [14, 15, 16, 17, 18, 19, 20, 21] and see references therein. The mathematical method is the Branin equation, an autonomous system of differential equations. It is singular at the VRI point. In this paper, we search for that singularity by an empirical trial and error approach. Branches of NTs can also be defined by a variational integral [22, 23]. The ansatz is repeated in this paper, at least for the theoretical background of the method. Usually, a whole family of NTs connects minimum and TS of index one. Thus, there is no unique NT between a minimum and a TS. However, a unique, a so-called singular NT connects a VRI point with its adjacent stationary points. This NT can be found by a variational treatment. Nowadays, variational treatments reach a renovation in RP calculations [22, 23, 24, 25, 26, 27, 28, 29, 30, 31, 32]. In this paper, we will explore the calculus of variations [33] for NTs.

The mathematically simplest RP definition is the steepest descent from an SP, resulting in the well-known intrinsic reaction coordinate (IRC) of Fukui [34, 35, 36, 37, 38, 39]. Its usual use is in mass-weighted Cartesians [38]. This pathway is defined by an autonomous system of differential equations for a tangent vector along the curve searched for being the gradient of the PES. Its solution is unique because outside of stationary points the gradient is not zero. Therefore, no bifurcation can occur before reaching the next stationary point. Hence, no branching of PES valleys will be truly described by following the IRC, see the discussion in refs. [40, 41]. The unique character will also emerge in a variational approach [28].

Gradient extremals (GE) [9, 42, 43, 44, 45, 46] appear to represent curves which meet special VRI points. They form another approach for RP following [47, 48, 49]. Special VRIs are passed by GEs and can be detected by following the GE. But to follow a GE is much more complicated than the IRC, or than an NT. Nevertheless, GEs are better fitted to solve the valley branching problem than the IRC, by the determination of a GE bifurcation itself [45, 46]. However, other problems arise due to the occurrence of pairs of turning points instead of a branching point (BP) of the

curve [50]. Such turning points may interrupt the pathway between minimum and SP. Then, the GE curves often show some kind of avoided crossing [9, 40, 41, 33, 44]. With its many additional solution curves and turning points [46, 47, 48], this concept in its general form is not suited to be used as a routine program for the calculation of reaction paths and possible VRIs. In the light of the variational ansatz, GEs do not fit to this idea [22], in contrast to their name, "extremal".

The paper is organized as follows: The Sects. 2 and 3 repeat fundamentals of the theory of variations. That will be applied in Sects. 4 and 5 to IRC and NTs as an RP definition, including conjugate points and the exceptional role of the IRC for an SP, and the NT for a VRI. In Sect. 6 of applications, we propose an empirical method to a variational ansatz, and we develop some examples: VRIs on the PES of HCN and one interesting VRI on the PES of alanine dipeptide. We finally add a short conclusion.

2 Variational methods [33, 51]

2.1 The variational integral

Before we give the go-ahead, here are some basics. Let be $F(t, x_1, \ldots, x_n, z_1, \ldots, z_n)$ a function with continuous first and second partial derivatives with respect to all its arguments. We search an extremum of a functional of the form

$$I(u,v) = \int_u^v F(t, x_1(t), \ldots, x_n(t), x_1'(t), \ldots, x_n'(t)) dt \qquad (1)$$

that depends on n continuously differentiable functions $\mathbf{x}(t) = (x_1(t), \ldots, x_n(t))^T$ being the components of an RP, $\mathbf{x}(t)$, in an n-dimensional configuration space. We regard all vectors as column vectors. The prime $'$ is the derivation to t. Note that I is a one-dimensional integral. The boundary conditions of the RP are

$$(x_1(u), \ldots, x_n(u))^T = \mathbf{U}, \text{ and } (x_1(v), \ldots, x_n(v))^T = \mathbf{V}.$$

These are usually the coordinates of minimum and SP, or of two adjacent minimums, or of two adjacent SPs, and $t \in R[u, v]$ is the curve parameter. Be $K \subset [u, v] \times \mathbf{R}^n$ a simple connecting region that contains the points $(u, \mathbf{U})$ and $(v, \mathbf{V})$. The set

$$\Gamma := \left\{ \gamma : t \mapsto \mathbf{x}(t) \in K | \mathbf{x} \in C^1[u, v], \mathbf{x}(u) = \mathbf{U}, \mathbf{x}(v) = \mathbf{V} \right\}$$

should contain all continuously differentiable paths between $\mathbf{U}$ and $\mathbf{V}$. Vector $\mathbf{x}$ is the representation of the RP $\gamma : t \mapsto \mathbf{x}(t)$. With $\mathbf{U}$ and $\mathbf{V}$ given, the task is to find a minimum of Eq. (1) over Γ, thus of $I(u, v)$. It is named the *simple fixed endpoint problem in the calculus of variations*.

The vectors **x** which belong to $\gamma \in \Gamma$ are named admissible. We define the two norms for $\mathbf{x} \in C^1[u, v]$

$$\|\mathbf{x}\|_0 := \sup_{t \in [u,v]} |\mathbf{x}(t)|,$$

and

$$\|\mathbf{x}\|_1 := \sup_{t \in [u,v]} |\mathbf{x}(t)| + \sup_{t \in [u,v]} |\mathbf{x}'(t)|. \qquad (2)$$

We name $\gamma^* \in \Gamma$ with the corresponding pathway $\mathbf{x}^*$

(i) *weak minimum* of (1), if an $\varepsilon > 0$ exists, that for all admissible **x** with $\|\mathbf{x}^* - \mathbf{x}\|_1 < \epsilon$ it holds $I(\mathbf{x}^*) \leq I(\mathbf{x})$.
(ii) *strong minimum* of (1), if an $\varepsilon > 0$ exists, that for all admissible **x** with $\|\mathbf{x}^* - \mathbf{x}\|_0 < \epsilon$ it holds $I(\mathbf{x}^*) \leq I(\mathbf{x})$.

Remark Strong minimum implicates weak minimum; but vice versa it does not hold, in general.

2.2 Necessary condition for extremals

The necessary condition for a curve $x_i = x_i(t)$, $i = 1, \ldots, n$, to be an extremal of the functional (1) is the system of Euler equations where we use subscripts to denote differentiation

$$F_{x_i} - \frac{d}{dt} F_{x'_i} = 0, \quad i = 1, \ldots, n. \qquad (3)$$

The integral curves of Euler equations are called *extremals* in mathematics in the field of the variational calculus.

2.3 Sufficient conditions for a (weak) minimal extremal

An important kind of points in variational theory is the following definition [33]: If a curve is an extremal of Eq. (1), starting at any point **U**, and a second "neighboring" extremal of Eq. (1), also starting at **U**, intersects the first curve in a next point, say point **W**, then the intersection point is called *conjugate point* (CP).

Example On a sphere, the meridians through the poles are the great circles with the shortest arclength but the poles are CPs because the extremals intersect there.

Besides the condition of the Euler equations, there are two further conditions for a weak minimum:

(i) The first conditions of a curve $\mathbf{x}(t)$ to be an extremal is the Jacobi condition that the curve does not have to contain CPs.
(ii) The second is the Legendre condition of positive definiteness of the second variation, of the matrix $F_{x'x'}$.

2.4 Sufficient conditions for a strong minimal extremal

A neighborhood of γ^* may be $U_\epsilon = \{\gamma \in \Gamma : \|\mathbf{x}^* - \mathbf{x}\|_0 \leq \epsilon\}$. There we define a vector field

$$\mathbf{x}' = \psi(t, \mathbf{x}) \qquad (4)$$

with $\psi \in C^1(K)$. We name it *field of extremals* of K, if every solution $\mathbf{x}(t)$ of (4) is also a solution of the Euler equations (3).

Remark:

(i) A field of extremals $\in C^1(K)$ is a family of extremals, where through every point of K goes exactly one extremal.
(ii) If we have an extremal, γ^*, of Eq. (1), which is additionally a trajectory of the field of definition (4), we say γ^* is embedded in the field (4).

The criteria of a weak extremum implicate the embedding of the extremal, $\mathbf{x}(t)$. A condition for a strong minimum is formulated by the *Weierstraß E-function*

$$E(t, \mathbf{x}, \psi, \mathbf{w}) := F(t, \mathbf{x}, \mathbf{w}) - F(t, \mathbf{x}, \psi) - (\mathbf{w} - \psi)^T F_{\mathbf{x}'}(t, \mathbf{x}, \psi). \qquad (5)$$

If it holds $E(t, \mathbf{x}, \psi, \mathbf{w}) \geq 0$ for all points $(t, \mathbf{x}) \in K$ and all finite vectors **w**, then γ^* is a strong minimal extremal of the variational problem (1).

3 Variational analysis of IRC and of NTs

The adiabatic PES of the molecular system of observation, $E(\mathbf{x})$, is the basis of our treatment. We use the Born-Oppenheimer approximation. We assume the PES is given by a scalar function of the coordinates of the molecule at every point of interest. Let K be the subset of $\mathbf{R}^n$ which we use for the *configuration space* of the PES. Let $\mathbf{x} = (x_1, \ldots, x_n)^T \in K$. The configuration space of a molecule is restricted. The function $E(\mathbf{x}) : K \to \mathbf{R}$ is an n − dimensional surface over K. The set $E_c = \{\mathbf{x} \in K, E(\mathbf{x}) = c\}$ is named *equipotential hypersurface*. We assume at least a twofold differentiability of the PES for practical reasons. The vector of first derivatives $\mathbf{g} : K \to \mathbf{R}^n$ with

$$\mathbf{g}(\mathbf{x}) = \left(\frac{\partial E}{\partial x_1}(\mathbf{x}), \ldots, \frac{\partial E}{\partial x_n}(\mathbf{x}) \right)^T \qquad (6)$$

is the *gradient*.

The second derivatives of E form the *Hessian* matrix $\mathbf{H}(\mathbf{x}) \in \mathbf{R}^{n \times n}$

$$\mathbf{H}(\mathbf{x}) = \left(\frac{\partial^2 E}{\partial x_i \partial x_j}(\mathbf{x}) \right)_{i,j=1}^n. \qquad (7)$$

The Hessian is symmetric. The *adjoint matrix* $\mathbf{A}$ of the Hessian matrix $\mathbf{H}$ is defined as $((-1)^{i+j} m_{ij})^T$ where m_{ij} is the minor of $\mathbf{H}$ obtained by deletion of the ith row and the jth column from $\mathbf{H}$, and taking the determinant. The adjoint matrix satisfies the relation

$$\mathbf{H}\mathbf{A} = det(\mathbf{H})\mathbf{I}_n, \tag{8}$$

$det(\mathbf{H})$ is the determinant of $\mathbf{H}$, and $\mathbf{I}_n$ is the unit matrix. A *stationary point* is where the gradient is zero

$$\mathbf{g}(\mathbf{x}) = 0, \tag{9}$$

like in minimums and SPs of any index. A *valley-ridge inflection point* (VRI) is a point where

$$\mathbf{A}(\mathbf{x})\mathbf{g}(\mathbf{x}) = 0, \quad \text{but} \quad \mathbf{g}(\mathbf{x}) \neq 0 \text{(usually)}, \tag{10}$$

see below for a deeper explanation.

3.1 Steepest descent: IRC

A pathway of wide interest is the IRC [36, 37], cf. also [38]. The steepest descent (SD) from the SP in (usually mass-weighted) Cartesian coordinates [52] is a simple definition of a reaction path, which is well known as the intrinsic reaction coordinate (IRC).

Using t for the curve parameter, a general *steepest descent* curve $\mathbf{x}(t)$ is defined by the system of vector equations in n dimensions

$$\mathbf{x}'(t) = -\mathbf{g}(\mathbf{x}(t)). \tag{11}$$

The SD system is a system of autonomous differential equations of the first order allowing an integration constant. Thus, its solution can start at an arbitrary initial point (where the gradient is not zero). The path (11) is given by the negative gradient of the PES for the tangent vector of the curve. But the potential force is the zero vector at stationary points, see Eq. (9). With the exception of the stationary points, the solution of the differential equation of the IRC is unique. Taking the IRC as a model, we may understand the definition of an RP by a system of autonomous differential equations like Eq. (11). The Jacobian matrix of $\mathbf{g}(\mathbf{x})$ is the Hessian. It is symmetric. Then, there is a simple possibility to transform such an RP definition from a differential equation into the variational form of Eq. (1). If $\mathbf{x}(t)$ is an RP, and the length $l(\mathbf{x}'(t))$ is given by

$$l(\mathbf{x}'(t)) = \sqrt{\mathbf{x}'(t)^T \mathbf{x}'(t)} = \sqrt{\sum_{k=1}^{n} x_k'(t)^2}, \tag{12}$$

then its variational formulation works with

$$F(\mathbf{x}, \mathbf{x}') = \sqrt{\mathbf{g}^T(\mathbf{x}(t))\mathbf{g}(\mathbf{x}(t))} \, l(\mathbf{x}'(t)), \tag{13}$$

because this F immediately fulfills the Euler equations [22]. One has the variational formula for the steepest descent [28, 29, 30, 31, 32, 53, 54].

$$I_{\text{SD}} = \int_u^v \sqrt{\mathbf{g}^T(\mathbf{x}(t))\mathbf{g}(\mathbf{x}(t))} \sqrt{\mathbf{x}'(t)^T \mathbf{x}'(t)} \, dt. \tag{14}$$

The extremal of $I_{\text{SD}} = \min$!, for $\mathbf{U} = \min$ and $\mathbf{V} = TS$, is the IRC. For integrants like Eq. (13), the matrix $F_{x'x'}$ has a zero determinant. The matrix is not positively definite. The second sufficient condition for a minimum is not fulfilled. Because the integrant of the task (14) has a positive first part, however, the extremal is a minimal curve [55].

3.2 Newton trajectory or reduced gradient [56]

A quarter of a century ago it was proposed to chose a driving coordinate along the valley of the minimum, to go a step in this direction, and to perform an energy optimization of the residual coordinates [57]. A combination of the distinguished coordinate method starting at the SP and steepest descent was also used [58]. Ten years ago, the method was transformed into a new mathematical form [1]. The chemically most important features of the PES are the reactant and the product minimum and the SP lain in between. These stationary points of the PES are characterized by the condition $\mathbf{g}(\mathbf{x}) = \mathbf{0}$. It is valid at extremizers of the PES, but single components of the gradient can also vanish in other regions of the PES. Using this property, a curve of points $\mathbf{x}$ can be followed which fulfills the $n-1$ equations

$$g_i = 0, \quad i = 1, \ldots, k-1, k+1, \ldots, n \tag{15}$$

omitting the $k-$th equation [1, 59]. This produces the $(n-1)$-dimensional zero vector of the *reduced gradient*; the method was subsequently called reduced gradient following. Eq. (15) means that the gradient points into the direction of the single x^k coordinate. The concept may be generalized by the challenge that any selected gradient direction is fixed

$$\mathbf{g}(\mathbf{x})/|\mathbf{g}(\mathbf{x})| = \mathbf{r} \tag{16}$$

where $\mathbf{r}$ is the selected unit vector of the search direction; and the corresponding curve is named *Newton trajectory*. The search direction may correspond to the start direction of a chemical reaction. The "reduction" of Eq. (16) is realized by a projection of the gradient onto the $(n-1)$-dimensional subspace that is orthogonal to the one-dimensional subspace spanned by the search direction $\mathbf{r}$. A curve belongs to the search direction $\mathbf{r}$, if the gradient of the PES always remains parallel to the direction of $\mathbf{r}$ at every point along the curve $\mathbf{x}(t)$

$$\mathbf{P_r}\mathbf{g}(\mathbf{x}(t)) = \mathbf{0} \tag{17}$$

where $\mathbf{P_r}$ projects with the search direction $\mathbf{r}$. This means $\mathbf{P_r}\,\mathbf{r} = \mathbf{0}$. A possibility to define $\mathbf{P_r}$ is [2, 60]

$$\mathbf{P_r} = \mathbf{I}_n - \mathbf{r}\mathbf{r}^T \tag{18}$$

where $\mathbf{I}_n$ is the unit matrix. This $\mathbf{P_r}$ is an $n \times n$ matrix of rank $n - 1$, because $\mathbf{r}$ is a column vector, $\mathbf{r}^T$ is a row vector, and their dyadic product is a matrix of rank 1. In Fig. 1, we show some NTs on a toy model. The surface $x^2 (x^2 - 2) + y^2$ with a double minimum at $(\pm 1, 0)$ is used, being the ideal case: it is found to occur in many systems. Additionally, the field of directions of the NT, Eq. (19), of $\mathbf{Ag}$ is shown by arrow heads. For two dimensions, the equipotential hypersurfaces, E_c, are only level lines.

NTs also have a definition by the Branin differential equation. The adjoint matrix $\mathbf{A}$ has to be used [61, 62, 63, 64, 65] to define an autonomous system of differential equations, similar to Eq. (11). For an NT curve $\mathbf{x}(t)$, where t is again the curve parameter

$$\mathbf{x}'(t) = \pm \mathbf{A}(\mathbf{x}(t))\mathbf{g}(\mathbf{x}(t)), \tag{19}$$

see also refs. [13, 50]. With the symmetric Hessian, the adjoint matrix $\mathbf{A}$ is also symmetric. However, the Jacobian matrix of the right hand side of Eq. (19) is non-symmetric, in general. A similar formula to (13) cannot be used. For an NT variational calculation, one may use a different variational functional by the general ansatz

$$F(\mathbf{x}, \mathbf{x}') = (\mathbf{x}' \mp A(\mathbf{x})\mathbf{g}(\mathbf{x}))^T (\mathbf{x}' \mp A(\mathbf{x})\mathbf{g}(\mathbf{x})). \tag{20}$$
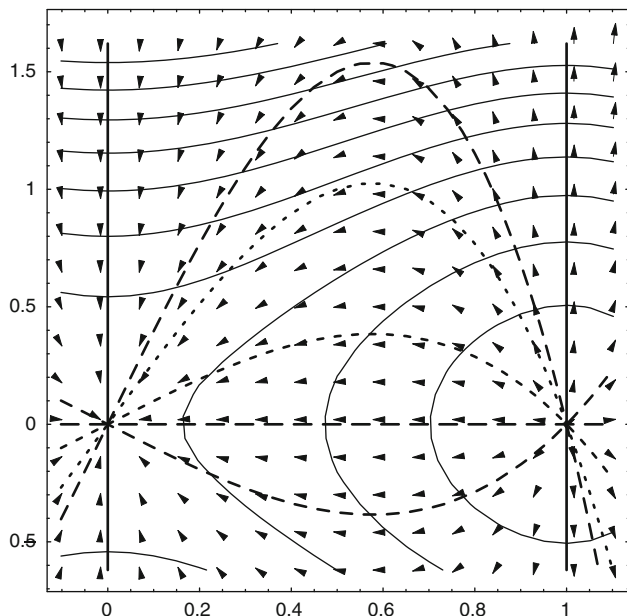

Fig. 1 Five NTs (*dashed curves*) of the family of NTs between minimum at (1,0) and SP at (0,0). Vector field $\mathbf{Ag}$. Level lines (*thin*) E_c

Of course, it is the differential equation (19) put into a variational functional. If the minimum of a variational integral with this integrant exists, it should be zero.

For an NT to a given direction, $\mathbf{r}$, there is a further functional recently given by Bofill [23]

$$F(t, \mathbf{x}, \mathbf{x}') = t\sqrt{\mathbf{g}^T\mathbf{g}}(\mathbf{r}^T\mathbf{x}') + E(\mathbf{x}), \tag{21}$$

where $\mathbf{g} = \mathbf{g}(\mathbf{x}(t))$, $E(\mathbf{x}) = E(\mathbf{x}(t))$, and $\mathbf{x}' = \mathbf{x}'(t)$.

4 Valley-ridge inflection points

If a valley pathway goes along the valley uphill, there are positive eigenvalues of the eigenvectors of the Hessian being orthogonal to the path, but usually some of the eigenvalues become smaller. Reaching a ridge, at least one corresponding eigenvalue is negative. Thus, we get for a VRI-point the

Definition Be $\mathbf{x}^{\mathbf{vri}} \in K$ with $\mathbf{g}(\mathbf{x}^{\mathbf{vri}}) \neq \mathbf{0}$, and be the eigenvalue zero, of the eigenvector of $\mathbf{H}(\mathbf{x}^{\mathbf{vri}})$, which is orthogonal to $\mathbf{g}(\mathbf{x}^{\mathbf{vri}})$. Then, we name $\mathbf{x}^{\mathbf{vri}}$ *Valley-Ridge Inflection Point* (VRI).

Be $\mathbf{u}^{\mathbf{zero}}$ the eigenvector of the Hessian with eigenvalue zero. At the VRI point holds

$$\mathbf{g}^{\mathbf{T}}\mathbf{u}^{\mathbf{zero}} = \mathbf{0}, \tag{22}$$

because, $\mathbf{g}(\mathbf{x}^{\mathbf{vri}})$ is orthogonal to $\mathbf{u}^{\mathbf{zero}}$. The gradient is not in the kernel of the Hessian, and it holds [66]

$$\begin{aligned} &\mathrm{rank}\big(\mathbf{H}(\mathbf{x}^{\mathbf{vri}})\big|\mathbf{g}(\mathbf{x}^{\mathbf{vri}})\big) \\ &= \mathrm{rank}\begin{pmatrix} \frac{\partial^2 E(\mathbf{x}^{\mathbf{vri}})}{\partial x_1 \partial x_1} & \cdots & \frac{\partial^2 E(\mathbf{x}^{\mathbf{vri}})}{\partial x_1 \partial x_n} & \frac{\partial E(\mathbf{x}^{\mathbf{vri}})}{\partial x_1} \\ \vdots & \ddots & \vdots & \vdots \\ \frac{\partial^2 E(\mathbf{x}^{\mathbf{vri}})}{\partial x_n \partial x_1} & \cdots & \frac{\partial^2 E(\mathbf{x}^{\mathbf{vri}})}{\partial x_n \partial x_n} & \frac{\partial E(\mathbf{x}^{\mathbf{vri}})}{\partial x_n} \end{pmatrix} < n. \end{aligned} \tag{23}$$

From the definition, we immediately obtain, that for VRI points $\mathbf{x}^{\mathbf{vri}}$ it holds

$$\mathbf{A}\big(\mathbf{x}^{\mathbf{vri}}\big)\mathbf{g}\big(\mathbf{x}^{\mathbf{vri}}\big) = \mathbf{0} . \tag{24}$$

To prove this [2], we use the eigenvectors, $\mathbf{u}^i$, of $\mathbf{H}$ and the λ_i the corresponding eigenvalues. With the equation of the eigenvalues $\lambda_i \mathbf{u}^i = \mathbf{H}\,\mathbf{u}^i$ follows after a multiplication with $\mathbf{A}$ from the left-hand side:

$$\lambda_i \mathbf{A}\mathbf{u}^i = \mathbf{A}\mathbf{H}\mathbf{u}^i = \det(\mathbf{H})\mathbf{u}^i = \left(\prod_{j=1}^{n} \lambda_j\right)\mathbf{u}^i . \tag{25}$$

Consequently, $\mathbf{A}$ has for $\lambda_i \neq 0$ the eigenvector $\mathbf{u}^i$ to eigenvalue $\left(\prod_{j=1}^{n} \lambda_j\right)/\lambda_i$. However, one eigenvalue at $\mathbf{x}^{\mathbf{vri}}$ is equal to zero per definition, it may be $\lambda_1 = 0$. Then, the eigenvectors $\mathbf{u}^2, \dots, \mathbf{u}^n$ of $\mathbf{A}$ also have the eigenvalue zero. We write $\mathbf{g}$ as a linear combination of the $\mathbf{u}^i$, thus,

$\mathbf{g} = \sum_{j=1}^{n} \xi_j \mathbf{u}^j$. Because the gradient $\mathbf{g}$ is orthogonal to $\mathbf{u}^1$ in $\mathbf{x}^{\mathbf{vri}}$, it is $\xi_1 = 0$, and we get the relation.

$$\mathbf{A}(\mathbf{x}^{\mathbf{vri}})\mathbf{g}(\mathbf{x}^{\mathbf{vri}}) = \xi_1 \left(\prod_{j=2}^{n} \lambda_j \right) \mathbf{u}^1 (\mathbf{x}^{\mathbf{vri}})$$
$$+ \sum_{i=2}^{n} \left[\xi_i \left(\frac{\prod_{j=1}^{n} \lambda_j}{\lambda_i} \right) \mathbf{u}^i (\mathbf{x}^{\mathbf{vri}}) \right]$$
$$= \mathbf{0}$$

which is Eq. (24). Every NT is a solution of Eq. (19). If $\mathbf{g} = \mathbf{0}$ different NTs can cross, or can confluent together. This is the case for all kinds of stationary points. There all different NTs with their different tangent directions can meet, because the gradient itself disappears there. A vector of zero length can "point" into every direction. However, if the gradient is not zero, different NTs cannot cross. This is the reason that only stationary points can be conjugate points of NTs. A more difficult situation emerges, if in Eq. (19) holds $\mathbf{Ag} = \mathbf{0}$. It is the condition of a VRI point. There more than one branch of a special NT can cross, of a so-called singular NT. This NT then bifurcates in the VRI point. The property is the fundament for this paper: we use it to calculate skew VRI points. We additionally assume that the cross of branches of the singular NT lies in a 2-dimensional plane, at least near the VRI point. Being with an approximating regular NT in that plan, or near to it, we can then search the VRI by an empirical procedure.

Note that an IRC from an SP downhill (accidentally) meets an VRI point only in very special cases, mostly dictated by symmetries [21]. Thus, we cannot employ the steepest descent to determine VRI points, in general [40, 41]. There is the border line between ridge and valley behavior [67] of the PES

$$\mathbf{g}(\mathbf{x})^T \mathbf{A}(\mathbf{x})\mathbf{g}(\mathbf{x}) = \mathbf{0}. \tag{26}$$

This line is sometimes crossed by the IRC, for example, if two adjacent SPs of first order lie on a PES, and we start the IRC at the upper SP. But the crossing point is generally not the VRI point. Of course, because of Eq. (24), the VRI point is always on this border line.

5 Conjugate points of extremals

5.1 IRC

To understand the deeper meaning of the CPs, we treat the catchment region of a minimum of the PES [68]. Catchment regions generate a partition of the n-dimensional configuration space K. Using the concept of SD curves, a catchment region $K_\mathbf{U}$ of the PES in K is defined as the collection of all those nuclear configurations $\mathbf{V}$ from where an infinitely slow, vibrationless relaxation path, as expressed by the SD, leads to a given critical point $\mathbf{U}$. The index of $\mathbf{U}$ is connected with the index of the critical point (the number of negative eigenvalues of the local Hessian matrix of the PES) at $\mathbf{U}$. The concept of catchment regions is closely related to ridges of the PES. Usually, an (n-1)-dimensional ridge system separates the catchment regions of two adjacent minimums, and every ridge ends below at an SP, cf. the 3D example of HCN [67]. An SP of index one is the TS that connects two adjacent minimums by the IRC.

A basic point in the theory of variational extremals [28] is the possibility of embedding the extremal curve under consideration in a family of neighboring curves that is fit to a field of directions. If the endpoint $\mathbf{V}$ of the extremal curve is in the catchment region of start point $\mathbf{U}$, then the original extremal can be embedded in a field. A field of curves is defined by the set of extremal curves cutting the hypersurfaces E_c transversally [28]. But still more explicitly, the cutting of SD curves to E_c is orthogonal. The set of extremal curves emerging from a central point $\mathbf{U}$ will constitute a field up to its conjugate points to the central point. In the present problem of SD curves flowing together into the point $\mathbf{U}$, which is a minimum, other SD curves may intersect this SD for the first time at the stationary points of the PES of a character saddle point, or maximum. These types of stationary points are the possible CPs with respect to central point $\mathbf{U}$ because there the gradient becomes zero again. Other points are not possible, because in other points the vector Eq. (11) for SD curves are unique. Thus, a CP can be a stationary point of a character saddle point of any index, or maximum on the PES. However, for saddle points with one negative eigenvalue, saddle points of index one, only one SD curve emerging form the central point $\mathbf{U}$ arrives at this type of stationary points. As a consequence, the first-order saddle points are not conjugate points with respect to the central point. This result is proved from a rigorous mathematical point of view in ref. [28], using the Jacobi equation associated to the variational problem under consideration.

For the IRC, no CP can exist. Different SD curves can only cross or confluent at saddle points. At maximums, as well as minimums, the field of SD curves starts, or confluents, at all [45, 69]. For a saddle of index 1 there is the IRC trough the SP, and the $(n - 1)$ corresponding ridge lines along the orthogonal directions do cross the curve. However, those ridge lines can never start at the minimum. All other neighboring curves do circumvent the SP in a hyperbolic kind. This is the reason why a variational minimization of the IRC works, if we fix the two startpoints to two minimums. From another point of view, seeing the SD curves from the two minimums, there are infinitely many SD curves that confluent there. However, only the IRC comes from the SP, and it is this single curve which

connects the two minimums. So to say, the IRC is a *singular* SD curve.

If an IRC is a "broken" extremal, like an IRC between two adjacent SPs of index one and a minimum, where the IRC first runs down between the two adjacent SPs, and then turns to the final minimum, the discussed relations are also in order, see ref. [30]. The case concerns ramified reaction valleys. Of course, an IRC connection between two SPs is only possible in special, symmetric cases of the PES [67].

SPs of an index higher than one, on the other side, are CPs of an adjacent minimum. It starts with SPs of index two which often are of chemical interest, too, cf. [70, 71, 72, 73, 74]. Consequently, an SD between an SP of index two and a minimum is not unique.

5.2 NTs

For NTs Eq. (19) is also unique in nonstationary points, if additionally $Det(\mathbf{A})$ of the adjoint matrix is not zero. But if $Det(\mathbf{A}) = 0$, we have a bifurcation point (BP) of an NT. The corresponding singular NT divides different families of NTs that connect different stationary points [13]. However, for NTs, the structure of the CP relation is quite more complicated than for SD curves. The reason is, adjacent stationary points like minimum and TS are conjugate points of NTs, see Fig. 1. Any NT without a BP connects stationary points with an index difference of one. Figure 1 shows a family of NTs between minimum and SP. It is to observe that the minimum is a repulsive stationary point, but the SP of index one is an attractive stationary point. The NTs fit the directions of the **Ag** field. Figure 1 shows that a minimization of a variational functional with integrant Eq. (20) between a minimum $\mathbf{U} = (1, 0)$ and a TS $\mathbf{V} = (0, 0)$ is not useful, because the solution is not unique. (Of course, that NT with the shortest pathlength, $L(u,v)$, can be used for an MEP [22]. It is here the line between 0 and 1 on the x-axis, the IRC). Only points $\mathbf{V}$ in the "NT-catchment region" of $\mathbf{U}$ being no stationary points are possibly to be uniquely calculated (at least theoretically) by the ansatz (20).

In contrast to the determination of stationary points being not possible by a variational calculation, NTs open the possibility for a new method to calculate all kinds of valley-ridge inflection (VRI) points. (The symmetric case has already been discussed [2, 6, 67]). The pattern of NTs around a VRI is the same like the pattern of SD curves around an SP, see Fig. 2. The analogy is: like the IRC is spanned over the SP of index one which is not a CP, because the IRC is the single curve which is going through the SP, a singular NT is going through a VRI which is not a CP either. A VRI point is the location which is crossed by the one, single NT which connects a minimum and an SP of index two, or which connects two SPs of index one. Every branch of the single NT separates families of
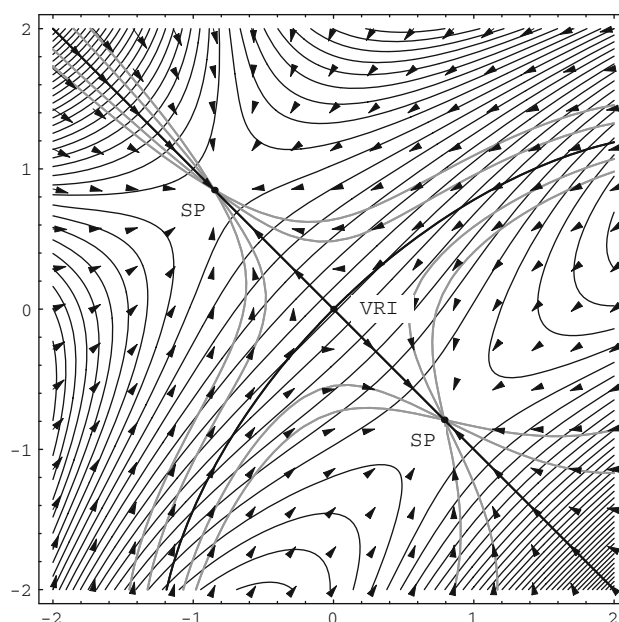

Fig. 2 Example of an **Ag** field around a VRI at zero, and some regular NTs (*gray lines*). The four branches of the singular NT through the VRI point are *bold curves*. Level lines are *thin*

hyperbolic NTs which connect different stationary points. So to say, the branch of a single NT is the border of catchment regions of different TSs. The corresponding regions of the PES are also named "reaction channels" to TSs [13]. In Fig. 2 we show the situation at a VRI point in a 2-dimensional example. The surface

$$E(x, y) = \frac{1}{2}(xy^2 - x^2y - 2x + 2y) + \frac{1}{30}(x^4 + y^4)$$

is used. The zero is the VRI point.

Finally, in this section, we prove the extremal character of NTs. Using functional (20), we get the Euler equations

$$F_{x_i} = 2(\mathbf{x}' \mp \mathbf{Ag})^T \left[\frac{\partial}{\partial x_i}(\mathbf{x}' \mp \mathbf{Ag}) \right] = 0 ,$$

$$\frac{dF_{x_i'}}{dt} = \frac{d}{dt} \left\{ 2(\mathbf{x}' \mp \mathbf{Ag})^T \left[\frac{\partial}{\partial x_i'}(\mathbf{x}' \mp \mathbf{Ag}) \right] \right\} = 0 .$$

Every NT is embedded in a field given by Eq. (19). To show that NTs are also strong extremals, we treat the Weierstraß condition (5). We first calculate $F_{\mathbf{x}'}$. It is with (20)

$$F_{x_i'} = \frac{\partial}{\partial x_i'} \sum_{j=1}^{n} \left(\left[x_j' \mp (\mathbf{Ag})_j \right]^2 \right)$$

$$= 2 \sum_{j=1}^{n} \left(\left[x_j' \mp (\mathbf{Ag})_j \right] \cdot \frac{\partial}{\partial x_i'} \left[x_j' \mp (\mathbf{Ag})_j \right] \right)$$

$$= 2 \sum_{j=1}^{n} \left(\left[x_j' \mp (\mathbf{Ag})_j \right] \delta_{ij} \right) = 2 \left[x_i' \mp (\mathbf{Ag})_i \right].$$

We get $F_{\mathbf{X}'} = 2(\mathbf{x}' \mp \mathbf{Ag})$. In relation (4), a field of extremals is given by

$$\psi(t, \mathbf{x}) = \pm \mathbf{A}(\mathbf{x})\mathbf{g}(\mathbf{x}).$$

It then holds

$$
\begin{aligned}
E(t, &\mathbf{x}, \psi, \mathbf{w}) \\
&= F(t, \mathbf{x}, \mathbf{w}) - F(t, \mathbf{x}, \psi) - (\mathbf{w} - \psi)^T F_{\mathbf{x}'}(t, \mathbf{x}, \psi) \\
&= |\mathbf{w}' \mp \mathbf{A}\mathbf{g}|^2 - \underbrace{|\psi \mp \mathbf{A}\mathbf{g}|^2}_{=0} - 2(\mathbf{w} - \psi)^T \underbrace{(\psi \mp \mathbf{A}\mathbf{g})}_{=\mathbf{0}} \\
&= |\mathbf{w}' \mp \mathbf{A}\mathbf{g}|^2 \geq 0
\end{aligned}
\tag{27}
$$

for finite vectors $\mathbf{w}$. NTs between a minimum $\mathbf{U}$ and a variable end point $\mathbf{V}$ are strong minimums of (1). Especially, between a stationary $\mathbf{U}$ and an adjacent VRI point is only one NT; and it is a strong minimal.

6 Empirical calculation of VRIs by NTs

In the past, the method of Allgower and Georg [75] was the method of choice for following an NT [2, 48, 76]. From the simple definition Eq. (17), a tangent was determined, by differentiation to a curve parameter. A predictor step was done along the tangent, and a corrector step by the Newton method was added, to find back to the true NT. Along the arguments of ref. [75], the venerable path following should also work for a curve with a bifurcation point (BP), but the convergence region of the corrector step could become smaller near the BP. There should be a cone of convergence with a tip at the BP. For 2-dimensional toy surfaces, the method works, indeed [77]. There are VRI points only, of "dimension" zero. However, for more than two-dimensional problems, the usual case in theoretical chemistry, there may emerge manifolds of VRI points [2, 6, 67]. It is expected that different "cones of convergence" of different neighbor NTs to different VRIs will overlay each other. The corrector to the current NT may diverge (long before the VRI) because the Hessian of the PES has a zero eigenvalue, or a very small eigenvalue, in a larger tube of neighborhood of the VRI of interest. In test calculations, we observed this behavior. There can be a region around a VRI point where the corrector step could not converge. It tries to converge, but from step to step, it hops through a larger region, and it finds at least a branch of the NT far behind the VRI, not the VRI itself. On the next branch, it can continue with convergent steps. The problem concerns the traditional predictor-corrector method [2, 76], as well as any chain method, where the initial "predictor" points are usually farther away from the searched NT [7, 78].

The way out is the direct use of Eq. (19) without a corrector step. We can discretize the differential equation (19) to a difference equation, and can do an Euler-Branin step along the direction of $\mathbf{A}\mathbf{g}$ which is also the tangent of an NT

$$\mathbf{step}_k = \pm p_l \mathbf{A}(\mathbf{x}_k)\mathbf{g}(\mathbf{x}_k)/|\mathbf{A}(\mathbf{x}_k)\mathbf{g}(\mathbf{x}_k)| \tag{28}$$

where p_l is the step length.

Note that the differential geometry (cf. [38, 56, 79, 80]) of such a step in curvilinear, internal coordinates is especially simple: $\mathbf{g}$ is a covariant vector, $\mathbf{H}$ is a two-fold covariant matrix, its quasi-inverse $\mathbf{A}$ is a two-fold contravariant matrix, and the product $\mathbf{A}\mathbf{g}$ has the contravariant form of the tangent step. (We use for $\mathbf{H}$ here only the direct second partial derivatives, but not the full covariant form with Christoffel symbols [56, 81, 82]. Nevertheless, this simplification works).

Usually, a regular NT turns aside with a strong curvature before the VRI point, see Fig. 2. If we initially do not have met the singular NT which exactly leads to the VRI point, we may follow a regular NT with predictor steps only, by steps along Eq. (28). But the NT is curved and predictor steps may diverge from it. However, if the regular NT is already near the 2-dimensional plane of the singular NT, then the "errors" of the predictor will point nearer to the VRI point than a truly corrected NT. To even leave out the corrector is a positive action here, in the case of the search for the VRI point, or its singular NT.

We follow the strategy "**SkewVRI**":

(i)   Choose chain length, n, step length, p_l, start point $\mathbf{x}_0$, start direction $d_i = \pm 1$ in Eq. (28), start index $i = 0$, and initial guess of the VRI point $\mathbf{v}_0$.

(ii) Determine the nodes $\mathbf{y}_{k,i}$ with $k = 1, \dots, n$ of a quasi-NT beginning in $\mathbf{y}_{1,i} = \mathbf{x}_i$ by

$$\mathbf{y}_{k+1,i} = \mathbf{y}_{k,i} + \mathbf{step}_k \tag{29}$$

using Eq. (28) with step length p_l and d_i.

(iii) Determine n-long straight further test chains of nodes $\mathbf{z}_{l,k,i}$ with $l = 1, \dots, n$ between every node $\mathbf{y}_{k,i}$ of (ii) and the VRI guess $\mathbf{v}_i$.

(iv) Determine on every test chain of (iii) the node $\mathbf{z}_{l,k,i}$ where $|\mathbf{A}\mathbf{g}|$ is minimal. Select the most minimal node of all chains over l and k to be the new $\mathbf{v}_{i+1}$.

(v)   Prove by any convergence criterion the convergence of $\mathbf{v}_{i+1}$, or the smallness of $|\mathbf{A}\mathbf{g}|$ at $\mathbf{v}_{i+1}$, to iterate further, or to stop the procedure.

(vi) Use the last node $\mathbf{y}_{n,i}$ of (ii) for a new start point $\mathbf{x}_{i+1}$, reverse the start direction by $d_{i+1} = -d_i$, and go to (ii) with $i = i + 1$.

The code is broken up into a number of FORTRAN programs, which communicate with external data files. We use program parts which deliver the input data to GAMESS-US, and other program parts which read out gradient, Hessian, and B-matrix for the internal metric from the GAMESS output file. The GAMESS-US is activated by a system call, correspondingly. Of course we also need programs for the following of a quasi-NT (step ii) and the

minimum search (step iii). The programs are downloadable from the web page [83].

Remarks In step (ii) we may also use the traditional predictor-corrector method [2] for an NT, if the corrector works well. In this case, we additionally need a search direction: the gradient at $\mathbf{v}_i$.

It is a good choice if the first guessed VRI is behind the true VRI seen from the nodes of the start chain.

In step (iii), we often only used the last 4 or 6 nodes before the guessed VRI, thus $\{\mathbf{z}_{n-6,k,i}, \ldots, \mathbf{z}_{n,k,i}\}$, to economize computing time. Of course, the number of nodes of the chains in steps (ii) and (iii) can also be different.

If one had a good choice of initial values and of the guessed VRI, the method may converge to the VRI point.

6.1 Example: HCN, cf. [67]

Calculations of gradient, Hessian, and **B** matrix for the metric have been carried out with the Gamess-US [84, 85] suite of programs for a PC employing the standard 6-31G** basis set. We use in the route section of the input file:

```
$CONTRL SCFTYP=rhf EXETYP=binv COORD=zmt
        NZVAR=3    RUNTYP=optimize    $END
$BASIS  GBASIS=n31 NGAUSS=6 NDFUNC=1 $END
$STATPT HESS=calc  NSTEP=1    NPUN3
        NPRT=-2    DXMAX=0.00001      $END
$FORCE  METHOD=analytic PRTIFC=.true. $END
```

It should be noted that the aim of the example was to demonstrate the VRI calculations and not to determine quantitative results. In this case, the calculations would have to be repeated with higher-level quantum mechanical basis sets. The RHF calculations used here deliver gradient and Hessian in internal z-matrix coordinates which we directly use in our program. (The Christoffel symbols in a fully correct covariant description of the Hessian are ignored).

The first example is the dissociation of the N-atom from the SP structure. Figure 3 shows the VRI point in the configuration space of HCN, with CN-distance and CH-distance in Å , and angle α between H–C–N in degree. (In the Figures, α is divided by 90°). Gradient and Hessian are used from GAMESS-US in *au*, thus distances in Bohr, angles in Radian. The branch between the SP and the VRI point is a ridge, its continuation to dissociation is a valley. The two bifurcating branches are the valley lines to the SP of a linear C–H–N (which is not fully calculated), or to the HCN minimum which is above the Figure (not shown). Included in Fig. 3 is the valley line from HNC minimum to the SP, the full line. For the calculation of the VRI point, we only need two runs of the program "SkewVRI". We start with a guessed VRI from ref. [67], there it is calculated by following gradient extremals. (For the triatomic
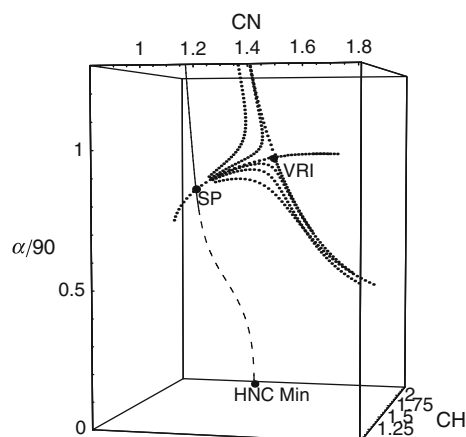

Fig. 3 Singular NT (*dots*) which meets the VRI point of an N-dissociation from HCN saddle in the 3-dimensional configuration space of internal coordinates. The singular NT connects SP and VRI point. There are also regular NTs (*dots* also) turning off the VRI region. The full line (*left* and *below*) is the valley line of the isomerization

HCN, gradient extremals are easy to calculate. For larger molecules, it becomes very difficult). A first run with the written "SkewVRI" method results in the two left and lower branches, a second run results in the two right and upper branches of the singular NT through the VRI point at (CN = 1.469, CH = 1.126, α = 87.543). The reached minimum of |**Ag**| is 2.8 e^{-6}*au*. The predictor steplength p_l used is 0.02 and 0.014Å. Additionally shown are four regular NTs, calculated by the traditional predictor-corrector method [2]. They are started at a point of the singular NT near the SP, however, the search direction is disturbed by $\pm\,0.01au$, of the CH-component, or of the α-component, correspondingly, against the search direction of the VRI point. Thus, the four NTs start on a "tube" around the singular NT.

The calculation of the VRI point is very easy, here. We think that it is a more or less singular point, not included in a one-dimensional manifold of VRI points. One could also use a (more correct) predictor-corrector method instead of pure predictor steps. If the N-atom leaves the SP structure, the H-atom distance to C is quasi fixed, as well as the H-angle. Only the N-distance determines the VRI point on the PES.

The meaning of the VRI point may be the decision for an incoming N atom (in Fig. 3 from the right hand side at α ≈ 90°) feeling an isolated CH diatom: goes it along a valley to the linear HC-N minimum, or goes it along a valley to a hypothetical N-HC linear SP of index 2 structure, or goes it before along a ridge in between to the SP? Compare Fig. 10 of ref. [67]. (From point of view of NTs, there is no direct regular NT to the HNC minimum). A similar decision has a dissociating N atom from the TS of HCN: it can leave the ridge from SP and dissociate, or it
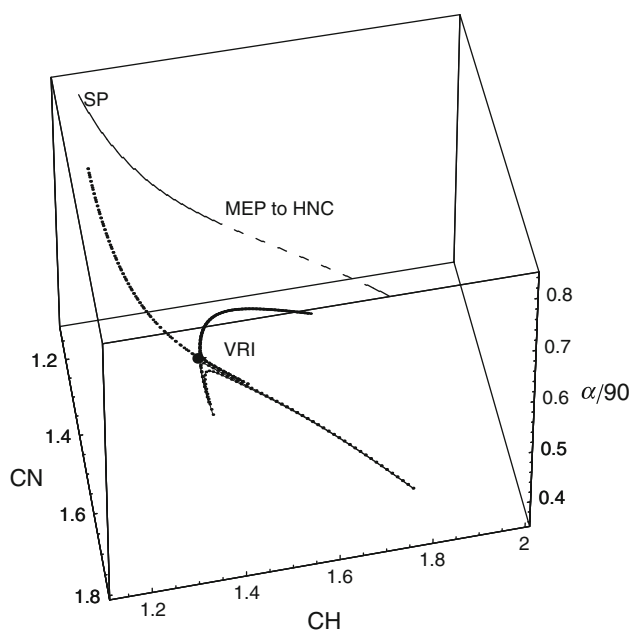
Fig. 4 A start NT (from SP), a regular NT around, and 4 branches of the singular NT through the VRI point, which emerges if the H-atom dips into the C≡N bond. In the rear is the valley line between SP and HNC minimum (*full line*). CN and CH axes are in the ground plane, the α axis points up
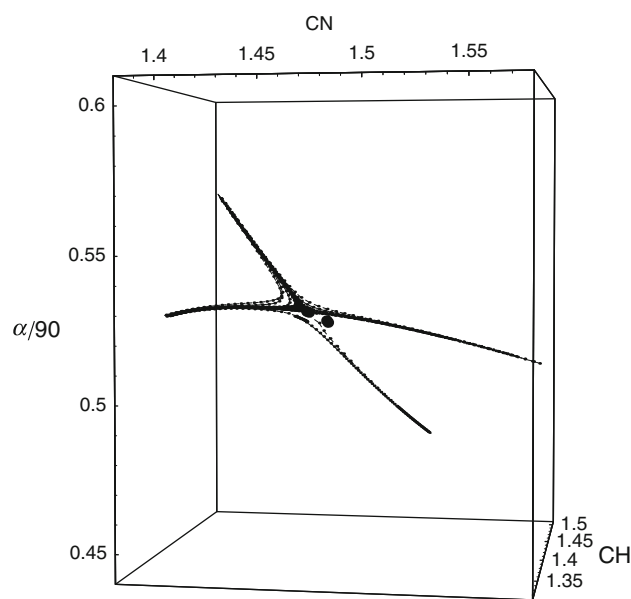

Fig. 5 Some regular NTs, as well as the singular NT through a further VRI point near the one of Fig. 4, which is here a little right below of the central VRI point. The NTs are calculated by predictor steps only

can go back along the other two valleys. Of course here is a free way to HNC minimum. The bifurcation of the NTs from TS to HNC or to C–H–N is the next example. (Note: NTs are not dynamical trajectories).

The second example is the pathway where the H-atom is coming from the SP structure and directly dips into the energy mountains of the C≡N triple bond. We find a whole region where the corrector does not work. However, before discussing that, we describe in Fig. 4 a VRI point at the "border" of the difficult region. It can be (by stock of luck) found with usual predictor-corrector steps [2], starting near the SP. Again, a guess of the VRI point of ref. [67] is used, at (CN = 1.455, CH = 1.351, α = 47.894), together with the search direction, **r**, the gradient direction at the guessed VRI. After the initial NT, a new guess of the VRI and its gradient is used for the next, regular NR. Using the regular NT that turns aside before the VRI point, the next search for the |**Ag**| minimum already results in a very good approximation. It is demonstrated by four branches of the singular NT which meet at the VRI point. It is at (CN = 1.475, CH = 1.359, α = 47.380) with an |**Ag**| minimum of $8.8\,e^{-5}au$. The branch in front of the Figure is a ridge of an incoming triple of the three single atoms H,C, and N. It leads downhill to the VRI point. Here, the branching takes place. The branch behind the VRI in the center is the valley NT leading from VRI downhill to the HNC minimum at (CN = 1.154, CH = 2.139, α = 0). (It is not fully calculated).

The usual situation in the region a little above of that VRI is that corrector steps do not converge. We have to use the "SkewVRI" method proposed here, by using ±**Ag** predictor steps only. An often well working choice is to start at the guessed VRI, calculate the first branch nodes with a small steplength, and do the further iterations with the double steplength. It makes that regular NTs smoothly go around before the VRI point or that the singular NT jumps over the VRI. The system of NTs shown in Fig. 5 is determined in this kind. It iterates into a further VRI point at (CN = 1.461, CH = 1.373, α = 47.662) with a minimum of $3.8e^{-7}au$. Not shown is a further VRI point found in another calculation at (CN = 1.463, CH = 1.371, α = 47.644) with an |**Ag**| minimum of $6.1\,e^{-6}au$. It is to guess that there is a "line" of VRIs. The four branches of the singular NT starting at the VRI are: The upper branch in Fig. 5 is the ridge line going from VRI downhill to the SP. The left branch is the valley line going downhill to the HNC minimum, (to the two branches, where no gradient extremal exists which could correspond to the NTs, see ref. [67]). The lower branch is the ridge line going uphill to the threefold dissociation of H,C, and N. The right branch is a ridge line (of index two) uphill in the direction to the linear N-H-C SP structure. It is at (CN = 2.111, CH = 1.0, α = 0), at very high energy, and the index is also two. Of course, always the beginning of the branches at the VRI is calculated.

A next, very strange case is the dissociation of the H-atom from the SP structure. In the region with a CH distance larger than 1.8Å, there it is totally unpromising
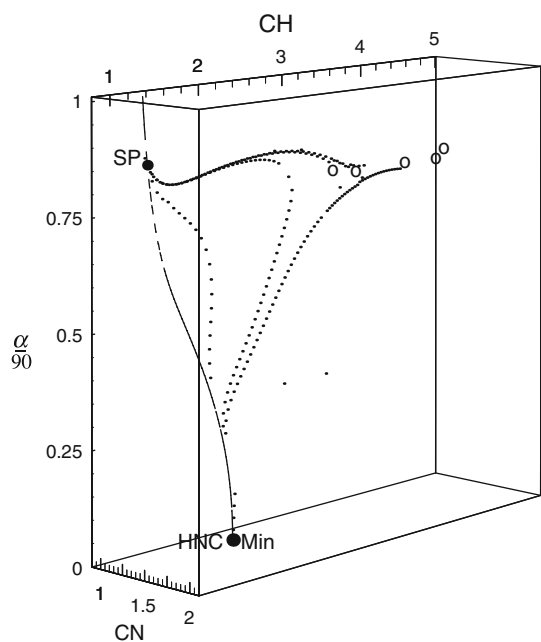
Fig. 6 HCN: some regular quasi-NTs (*dots*) which surround quasi-VRI points (*empty circles*) of an H-dissociation from the SP structure. The full line is the valley line from SP to HNC minimum. The NTs are calculated by predictor steps only, see text

to use the corrector of the traditional method. Only **Ag**-predictor steps work. We have consequently used the method "SkewVRI" proposed above. Again, a guess of the VRI point of ref. [67] is used, at (CN = 1.186, CH = 3.329, α = 70.994). There we find |**Ag**| = 8.4 $e^{-5}au$. The result of some calculations is depicted in Fig. 6. Different quasi-VRIs are shown by empty circles, because we find a "development" along Fig. 6 from left to right. An NT crosses the first, most left, guessed VRI point, it may be a regular NT. From there, the next VRI guess is iterated; the system of shown regular NTs surrounds that second VRI point. It is at (CN = 1.189, CH = 3.619, α = 70.125). There we find a smaller |**Ag**| = 3.8 $e^{-5}au$. There are regular NTs, but there is also an NT which in good approximation can be considered as a singular one, through the point. By other calculations, we find the other circles of Fig. 6. with CH distances of 4.25, 4.66, and 4.77Å. There the |**Ag**| minimum further decreases along 1.1 e^{-5}, 8.7 e^{-6}, and to 7.9 $e^{-7}au$. The (theoretical) question emerges: what is the VRI point? It is to guess that there is a "long cloud" of quasi-VRIs. It is clear that the function |**Ag**| decreases very slowly over a very large region of increasing CH-distances. The decision for a VRI may strongly depend on the convergence criterion. From a practical point of view, we may localize the VRI situation around CH = 3.5 Å. However, long before, near CH = 1.8 Å, a normal calculation of NTs by predictor-corrector steps breaks down by a very small determinant of the K-matrix, see refs.[2, 48].

6.2 A higher dimensional example: alanine dipeptide

Alanine is one of the most common proteinogenic amino acids. We apply the VRI search to alanine dipeptide (Acetyl-L-Ala-NHMe),

$CH_3CO-NHCHCH_3CO-NHCH_3$.

Alanine dipeptide is our second example for a VRI point search. It is chosen because here the "SkewSearch" comes to its borderline. The molecule is already a little too large. In this section, we describe a problem which emerges for a molecule of 22 atoms. We use the same non-redundant internal coordinates and parameters like in ref. [7], as well as study the region between the two conformers C5 and C7ax. We use the same metric calculation described in ref. [7]. To avoid the difficulties with the two outer CH_3-groups of the molecule which sometimes do an enormous internal rotation, reported in ref. [7], we fix them. Then, we have to handle 58 remaining degrees of freedom. The fixing concerns *dih4*, the torsional angle between atoms (O4,C3,C2,H1), and *dih22* of (H22,C18,N17,C9), in the Chass et al. [86] numbering. (See Fig. 2 of ref. [7]). The fixing of two coordinates is a distortion; however, its gain is more than the problems which the two outer CH_3-groups would cause.

Calculations of gradient and Hessian have again been carried out with the Gamess-US [84, 85] suite of programs for a PC employing the standard 6-31G basis set. We use for the method:

```
$CONTRL SCFTYP=rhf NZVAR=60 EXETYP=ginvr
        RUNTYP=optimize     COORD=zmt
        NPRINT=1                      $END
$BASIS  GBASIS=n31 NGAUSS=6 NDFUNC=0   $END
$STATPT HESS=calc  DXMAX=0.00001
        NPRT=-2    NPUN=3    NSTEP=1   $END
$FORCE  METHOD=analytic PRTIFC=.true. $END
```

The *z*-matrix option is used to avoid redundant coordinates which would disturb the corrector step. NSTEP is set to one to get gradient and Hessian of the current point without an optimization. On the other hand, we have to use the optimize option to get these values, at all. Two coordinates, no. 6 being *dih4* and no. 60 being *dih22*, are fixed in the *z*-matrix; however, the Gamess-US uses the full dimension, $n = 60$, for the internal calculations. From the Gamess-US output file, we grasp the figures which we need in the SkewVRI procedure: (energy), gradient, Hessian matrix, and **B** matrix. In the output of gradient, Hessian matrix, and metric matrix g^{ij}, we delete the lines and columns, 6 and 60. (g^{ij} is built from the full **B** matrix of 60×66 dimension). The inverse metric g_{ij} is calculated with an SVD procedure [87] from metric matrix g^{ij} in 58 dimensions. The coordinates for the input are in Å and degree, but gradient and Hessian are calculated in the

(Bohr, Radian) system, especially in Hartry/Bohr, Hartry/Radian (gradient), or Hartry/Bohr^2, Hartry/Bohr*Radian, or Hartry/Radian^2 (Hessian), correspondingly.

To search and find the one singular NT to the VRI, we have to truly use the right metric. It is a stronger condition than the search of an SP starting in a minimum: there a full family of NTs leads to the SP. It is not important, really, which special regular NT we follow. However, for the singular NT, we have to exactly meet the search direction: the covariant gradient at the VRI point. In the example, we search for the VRI point between the C5 minimum, and the SP of index 2, the summit in Fig. 7. The underlying PES is optimized over a raster of points of (ϕ, ψ). All NTs are projected into the 2-dimensional plane of (ϕ, ψ), the torsional angles *dih*13, and *dih*17 [86].

A problem emerges in the calculation of the adjoint matrix **A**. Usually, the exactness to zero of the reduction projector applied to the predictor tangent is $\approx 10^{-19}$. On the other hand, the Hessian has only two eigenvalues larger than one, near the VRI, in the used (Bohr,Radian) system: so to say good values. But because many more values (56) are smaller than one, the determinant of **H** in the 58 dimensions used becomes around $\approx 10^{-35}$. A similar value has the determinant of the **K** matrix of the corrector. Nevertheless, the procedure *linsolve* works well for corrector and predictor of a usual NT following. However, the calculation of the adjoint matrix **A** from the Hessian by minors of **H** does not result in useful values by (probably) numerical cancellation of significant digits. Here numerical problems emerge: resulting entries of **A** are between $\approx 10^{-38}$ and $\approx 10^{-40}$, and the values of the vector **Ag** and of its norm become, more or less, erratical. Especially, the corresponding vector, **Ag**, is not parallel to the tangent from the predictor. We find a (rough-and-ready) way out of
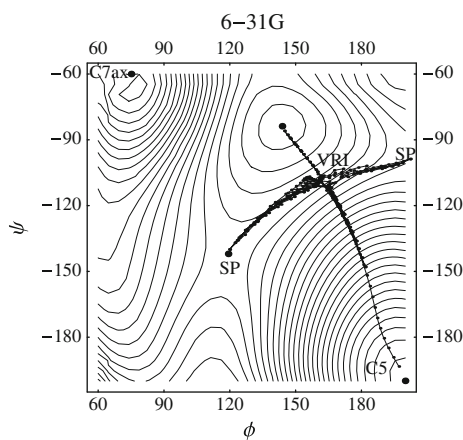
this numerical problem. For **A** only, we multiply the entries of the Hessian by a factor 4 (because $4^{58} \approx 10^{35}$, $\tilde{\mathbf{H}}$=4 **H**, and this compensates the smallness of the determinant).

Table 1 VRI point of alanine dipeptide near C5 minimum

|		
1.0823533	1.5076906	109.0854125
1.2297386	120.6150737	64.0
1.0815013	108.6200117	−52.7854714
1.0807919	113.3276565	−174.0747806
1.3551050	115.4819160	−116.3800443
1.4681739	127.5004933	179.0925717
1.5309121	103.5669621	**161. 5368811**
1.2337026	118.5015250	69.2084861
1.0839450	109.0386273	−86.3556218
0.9942629	117.5701266	10.9150013
1.5270619	114.4009734	35.5621857
1.0760130	110.2704005	−67.6612961
1.0842233	109.4652807	−187.3460581
1.0831225	112.0328517	51.2159897
1.3438684	118.4260894	**−106.8333517**
1.4548965	123.1346690	176.5693575
1.0823606	110.5592725	120.5810590
0.9900383	119.1582596	−1.4098970
1.0769551	108.6527121	0.9249162
1.0835450	110.5444637	−119.0

The *z*-matrix coordinates (in Å and degree) are in the order of Chass et al. [86]. (ϕ, ψ) are bold. Variables 6 and 60 are fixed

Table 2 Search direction (in Bohr and Radian) at the VRI point of Table 1. (ϕ, ψ) are bold

−0.00054	0.00549	0.00157
−0.01351	0.01918	−
0.0054	0.01328	−0.01765
0.01903	−0.02566	0.06135
−0.00144	−0.02998	−0.1122
−0.02567	0.1195	0.12004
−0.00466	−0.29166	**−0.2468**
0.00652	−0.04949	0.09877
0.00696	−0.07526	0.06663
0.00885	0.02561	0.01321
−0.04086	0.12001	−0.18274
0.01831	−0.0247	−0.01146
0.00332	−0.00721	0.04852
−0.02682	0.03109	−0.01739
0.07269	−0.27212	**0.54095**
0.01168	0.17525	−0.1179
−0.00625	−0.00695	0.06133
0.00363	−0.00076	0.08296
0.01316	−0.01758	0.04853
0.07244	−0.00505	−

Components 6 and 60 are not used

Fig. 7 Alanine dipeptide: some NTs (*connected dots*) which surround the VRI point between minimum C5 and the SP of index 2, and between two SPs of index one. NTs are calculated by predictor-corrector steps

Fig. 8 Alanine dipeptide: Four branches of the singular NT (*connected dots*) in different runs. They are started at the VRI point (*empty circle*). All four branches of the singular NT are found. Coordinates are the two torsional angles (ϕ, ψ) like in Fig. 7 measured in degree. All chains are projected into this plane
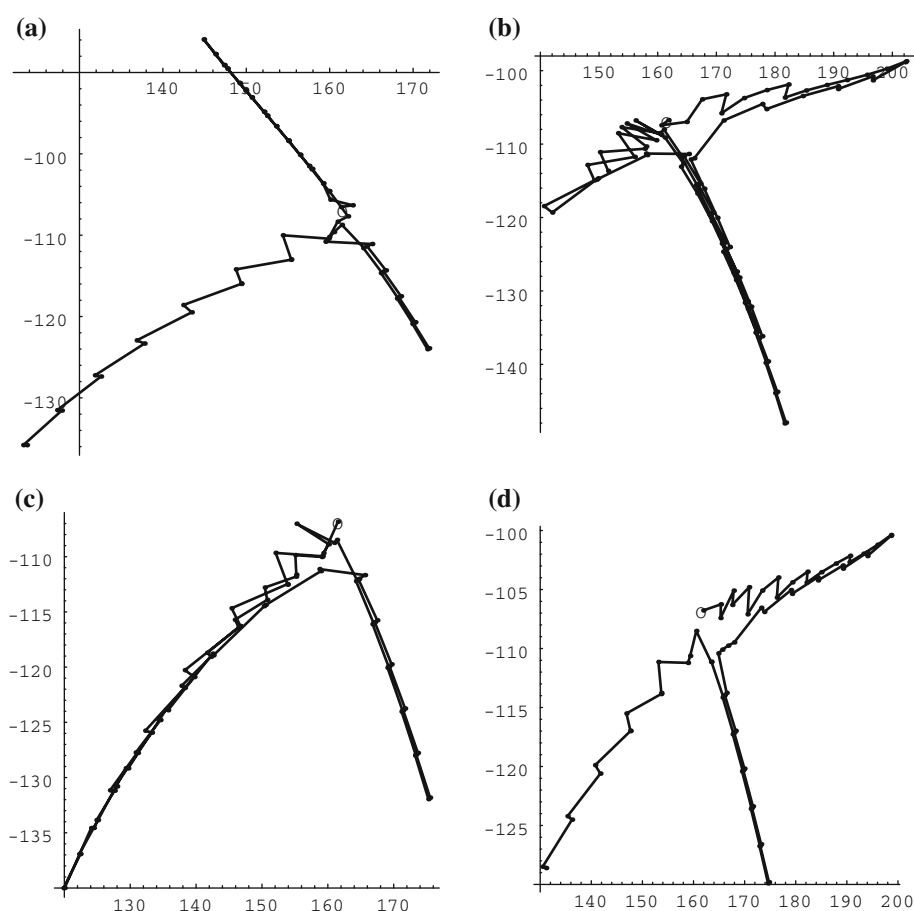
Then, the determinant of the shifted Hessian is near, or a little less than 1, in a neighborhood of the minimum C5. The operation results in a shifted adjoint matrix $\tilde{\mathbf{A}}$ calculated from $\tilde{\mathbf{H}}$. The task $|\tilde{\mathbf{A}}\mathbf{g}| \to$ min! is the same as before, but now the numerical handling is possible. We use the minimum for the decision in step (iv) of the "SkewVRI" strategy.

In our previous work [7] we could present some NTs that connect the minimums C5 and C7ax over the SP. There we guessed that there are VRI points because there takes place a bifurcation of some regular NTs. One of the BPs we try to obtain exactly in this work. We start with nodes of NTs coming near to the guessed VRI point. The initial search direction is the gradient of the guessed VRI. A start in C5 with a very mild threshold for the corrector delivers a chain of nodes, from which the SkewVRI method can begin to search the VRI minimum along the lines of procedures (iii) and (iv). We use chains of 12 nodes for the NTs, and for the minimum search in procedure (iv) we also take 12 nodes of every connecting line between nodes of the NT-chain, and the guessed VRI. However, we only take the last six points of every connecting line for the $|\tilde{\mathbf{A}}\mathbf{g}|$ minimum search. The found VRI is again used for a new run, to get a better one, and so on. The value of $|\tilde{\mathbf{A}}\mathbf{g}|$

along regular NTs is around 0.5 units, the reached minimum in the third test run already reaches 0.000 23 units, thus a reduction of the test value of 1 to 1/2 000. If one starts after a run at the new VRI, and calculates NTs forward and backward, one gets the cross of quite good branches of the singular NT. The final adapted VRI point is given by Table 1. The corresponding VRI direction is the gradient direction at the VRI given in Table 2. Comparing with the used search directions of ref. [7], here, not only the five active torsional angles are involved (of the C5 to C7ax transition described there), but, more or less, the full 58 dimensions are exhausted. In nine further coordinate directions, besides the (ϕ, ψ), are contributions larger than 0.1 units. At least, we find the "singular" NT through a VRI point of alanine dipeptide, see Fig. 8. The NTs rely on the first predictor step: (a) toward uphill, (b) toward downhill, (c) to the left, or (d) to the right-hand side. The threshold for the VRI minimum, 0.000 23 units, is not used at the beginning of every run, to do some more iterations. At least tree chains, forward and backward and backward again, are attempted in every run. The first chain uses a predictor step length of 0.2 units (Bohr,Radian), but every further chain uses 0.35 units. Usually, the minimum reached in the second iteration cannot become lower than

that of the first iteration. Then, the calculation stops after the next NT chain. Run (a), for example, has tested three chains. It needs 22 hours on a PC. Here in alanine dipeptide, we use the full predictor-corrector procedure in step (ii). The used threshold for the corrector along an NT chain is the small value of 0.000 1 units for the norm of the reduced gradient (thus Bohr,Radian). Along an NT, the method usually makes one, sometimes two corrector steps, sometimes it does not need the corrector, at all. This demonstrates that the following of the NTs works well. The predictor takes a good direction, and the corrector does the appropriate steps, then.

An inspection of the found singular NT of Fig. 8 will open the way to describe the 2-dimensional plane where the VRI point is located. The plane develops in any kind "skew" in the full 58 dimensions of all use degrees of freedom. (Fig. 8 is only a projection of the bifurcating NT in the known scheme of the (ϕ, ψ) coordinates). If one has such a plane through the VRI point, one may define two "normal coordinates" of the bifurcational event represented by the VRI point: one coordinate of the reaction direction which will bifurcate there, and one of the direction of the bifurcation itself. Like usual normal coordinates are a linear combination of the coordinates used, also the two bifurcational coordinates will be a linear combination of all coordinates. We guess that an ansatz to "know" this plane before the calculation will be a speculation. May be it can be supported a little by chemical intuition, c.f. another example [88]. The theory of NTs allows us to search quasi "ab initio" for the VRI plane in the full dimension of the molecules degrees of freedom. (Of course, we need a guess of the region of the configuration space where the VRI could be).

7 Conclusion

We use singular NTs to explore skew VRI points for HCN and alanine dipeptide. We find the singular NTs with an empirical variational scheme. It works.

References

1. Quapp W, Hirsch M, Imig O, Heidrich D (1998) J Comput Chem 19:1087
2. Quapp W, Hirsch M, Heidrich D (1998) Theor Chem Acc 100:285
3. Anglada JM, Besalu E, Bofill JM, Crehuet R (2001) J Comput Chem 22:387
4. Bofill JM, Anglada JM (2001) Theor Chem Acc 105:463
5. Crehuet R, Bofill JM, Anglada JM (2002) Theor Chem Acc 107:130
6. Hirsch H, Quapp W, Heidrich D (1999) Phys Chem Chem Phys 1:5291
7. Quapp W (2009) J Theor Comput Chem 8:101
8. Heidrich D (1995) The reaction path in chemistry, current approaches and perspectives. Kluwer, Dordrecht
9. Heidrich D, Kliesch W, Quapp W (1991) Properties of chemically interesting potential energy surfaces, lecture notes chem 56. Springer, Berlin
10. Laidler K (1969) Theory of reaction rates. McGraw-Hill, New York
11. Quapp W, Zech A (2010) J Comput Chem 31:573
12. Truhlar DG, Garrett BC (1980) Acc Chem Res 13:440
13. Hirsch M, Quapp W (2004) J Mol Struct(Theochem) 683:1
14. Bakken V, Danovich D, Shaik S, Schlegel HB (2001) J Am Chem Soc 123:130
15. Quadrelli P, Romano S, Toma L, Caramella P (2002) Tetrahedron Lett 43:8785
16. Ussing BR, Hang C, Singleton DA (2006) J Am Chem Soc 128:7594
17. Thomas JB, Waas JR, Harmata M, Singleton DA (2008) J Am Chem Soc 130:14544
18. Ess DH, Weeler SE, Iafe RG, Xu L, Çelebi-Ölçüm N, Houk KN (2008) Angew Chem Int Ed 47:7592
19. Tantillo DJ (2008) J Phys Org Chem 21:561
20. Hong YJ, Tantillo DJ (2009) Nature Chem 1:384
21. Yamataka H, Sato M, Hasegawa H, Ammal SC (2010) Faraday Discuss 145:327
22. Quapp W (2008) Theor Chem Acc 121:227
23. Bofill JM (2009) J Chem Phys 130:176102
24. Elber R, Karplus M (1987) Chem Phys Lett 139:375
25. Czerminski R, Elber R (1990) Int J Quant Chem S 24:167
26. Elber R (1996) In: Elber R (ed) Recent developments in theoretical studies of proteins. World Scientific, Singapore, p 65
27. Pratt LR (1986) J Chem Phys 85:5045
28. Crehuet R, Bofill JM (2005) J Chem Phys 122:234105
29. Aguilar-Mogas A, Crehuet R, Giménez X, Bofill JM (2007) Mol Phys 105:2475
30. Aguilar-Mogas A, Crehuet R, Bofill JM (2008) J Chem Phys 128:104102
31. Vanden-Eijnden E, Heymann M (2008) J Chem Phys 128:061103
32. Heymann M, Vanden-Eijnden E (2008) Comm Pure Appl Math 61:1052
33. Gelfand IM, Fomin SV (1991) Calculus of variations. Dover Publ Inc, Mineola, New York
34. Fukui K (1974) J Phys Chem 74:4161
35. Fukui K (1974) In: Daudel R, Pullman P (eds) The world of quantum chemistry. Dordrecht, Reidel, p 113
36. Fukui K (1970) J Phys Chem 74:4161
37. Tachibana A, Fukui K (1978) Theor Chim Acta 49:321
38. Quapp W, Heidrich D (1984) Theor Chim Acta 66:245
39. Garrett BC, Redmon MJ, Steckler R, Truhlar DG, Baldridge KK, Bartol D, Schmidt MW, Gordon MS (1988) J Phys Chem 92:1476
40. Schlegel HB (1994) J Chem Soc, Faraday Trans 90:1569
41. Quapp W (1994) J Chem Soc, Faraday Trans 90:1607
42. Basilevsky MV, Shamov AG (1981) Chem Phys 60:337; and 60:347
43. Hoffman DK, Nord RS, Ruedenberg K (1986) Theor Chim Acta 69:265
44. Quapp W (1989) Theoret Chim Acta 75:447
45. Sun J-Q, Ruedenberg K (1993) J Chem Phys 98:9707
46. Quapp W, Imig O, Heidrich D (1995) In: Heidrich D (ed) The reaction path in chemistry, current approaches and perspectives. Kluwer, Dordrecht, p137

47. Jensen F (1995) J Chem Phys 102:6706
48. Quapp W, Hirsch M, Heidrich D (2000) Theor Chem Acc 105:145
49. Quapp W, Bofill JM (2010) J Computat Chem submitted
50. Hirsch M, Quapp W (2004) J Math Chem 36:307
51. Moser J (2003) Selected chapters in the calculus of variations. Birkhäuser, Lect Math, ETH Zürich
52. Truhlar DG, Kupperman AJ (1971) J Am Chem Soc 93:1840
53. Olender R, Elber R (1997) J Mol Struc(Theochem) 398-399:63
54. Stacho LL, Dömötör G, Ban MI (2000) J Math Chem 28:241
55. Carathéodory C (1935) Variationsrechnung und partielle Differentialgleichungen erster Ordnung. Teubner, Leipzig
56. Quapp W (2003) J Theor Comp Chem 2:385
57. Czerminski R, Elber R (1990) J Chem Phys 92:5580
58. Steckler R, Truhlar DG (1990) J Chem Phys 93:6570
59. Williams IH, Maggiora GM (1982) J Mol Struct(Theochem) 89:365
60. Ulitzky A, Elber R (1990) J Chem Phys 92:1510
61. Branin FH (1972) IBM J Res Develop :504
62. Jongen HT, Jonker P, Twilt F (1987) In: Guddat J et al. (eds) Parametric optimization and related topics. Akademie-Verlag, Berlin, pp 209–300
63. Jongen HT (1990) In: Allgower EL, Georg K (eds) Computational solutions of nonlinear systems of equations. Amer Math Soc, Providence, p 317
64. Diener I, Schaback R (1990) J Optimiz Theory Appl 67:87
65. Diener I (1991) Globale Aspekte des kontinuierlichen Newton-Verfahrens. Habilitation, Göttingen
66. Gomulka J (1974) In: Towards global optimisation. Dixon LCW, Szegö GP (eds), North-Holland, p 96
67. Quapp W, Hirsch M, Heidrich D (2004) Theor Chim Acta 112:40
68. Mezey PG (1987) Potential energy hypersurfaces. Elsevier, Amsterdam
69. Ruedenberg K, Sun J-Q (1994) J Chem Phys 100:5836
70. Heidrich D, Quapp W (1986) Theor Chim Acta 70:89
71. Minyaev RM, Getmanskii IV, Quapp W (2004) Russ J Phys Chem 78:1494
72. Kim H-W, Zeroka D (2008) Int J Quant Chem 108:974
73. Ezra GS, Wiggins S (2009) J Phys A 42:205101
74. Haller G, Uzer T, Palacian J, Yanguas P, Jaffe C (2010) Commun Nonlinear Sci Numer Simulat 15:48
75. Allgower EL, Georg K (1990) Numerical continuation methods. Springer, Berlin
76. Hirsch M, Quapp W (2002) J Comput Chem 23:887
77. Schmidt B (2009) Bestimmung von Tal-Rücken-Umschlagpunkten auf Potentialenergieflächen mittels eines Variationsansatzes für Newtontrajektorien. Diplomarbeit, Mathematisches Institut, Universität Leipzig
78. Quapp W (2005) J Chem Phys 122:1
79. Quapp W (2004) J Math Chem 36:365
80. Quapp W (1995) In: Heidrich D (ed) The reaction path in chemistry, current approaches and perspectives. Kluwer, Dordrecht. p 95
81. Wales DJ (2000) J Chem Phys 113:3926
82. Quapp W (2001) J Chem Phys 114:609
83. Quapp W (2010) http://www.math.uni-leipzig.de/~quapp/Skew VRIs/
84. Schmidt MW, Baldridge KK, Boatz JA, Elbert ST, Gordon MS, Jensen JH, Koseki S, Matsunaga N, Nguyen KA, Su SJ, Windus TL, Dupuis M, Montgomery JA (1993) J Comput Chem 14:1347
85. Granovsky AA (2009) PC GAMESS, http://www.classic.chem.msu.su/gran/gamess
86. Chass GA, Sahai M, Law JMS, Lovas S, Farkas Ö, Perczel A, Rivail L-L, Csizmadia IG (2002) Int J Quant Chem 90:933
87. Vetterling WT, Teukolsky SA, Press WH, Flannery BP (1992) Numerical recipes in Fortran, the art of scientific computing, 2d edition. New York, Cambridge University Press
88. Sheppard AN, Acevedo O (2009) J Am Chem Soc 131:2530